SUBSURFACE STRUCTURES AT THE CHANG'E-3 LANDING SITE: INTERPRETATIONS FROM ORBITAL AND IN-SITU IMAGERY DATA. L. Qiao[1], Z. Y. Xiao[1, 2], J. N. Zhao[1] and L. Xiao[1], [1]Planetary Science Institute, China University of Geosciences, Wuhan 430074, China (le.qiao@cug.edu.cn), [2]Centre for Earth Evolution and Dynamics, University of Oslo, Postbox 1028 BlindernN-0315 OSLO Norway.

Introduction: Quantifying the subsurface stratigraphic and tectonic features of the Moon can provide key information for scientific mysteries concerning regional and global geology and evolutionary history of the Moon.

In December 2013, China's Chang'e-3 (CE-3) spacecraft, carrying the Yutu (Jade Rabbit) rover, successfully landed on the northern Mare Imbrium region [1]. The rover equipped a radar system that could reveal subsurface structures in unprecedented details, which would be indicative for regional and global geological evolutionary history of the Moon [2, 3]. To assist the interpretation of the CE-3 radar data, here we quantify the subsurface structures at the CE-3 landing site using both orbital and in-situ imagery data based on regional geology, cratering scaling, and morphological study.

Geological Setting of the CE-3 landing site: The CE-3 spacecraft landed on the continuous ejecta blanket of a crater ~500 m in diameter (C1 crater) in northern Mare Imbrium region. Two sets of mare basalts have been identified at the landing area: the Eratosthenian (~2.5 Ga) moderate-titanium basalt at the landing site and the Imbrian (>3.3 Ga) low-titanium basalt in the north [1]. The northern Imbrian basalt unit was predicted to have existed beneath the Eratosthenian basalt at the CE-3 site. During the interval of the two lava-filling events, a regolith layer formed on the top of the underlying Imbrian basalts. Another regolith layer was accumulated on the surface of the Eratosthenian basalts after the basalt deposition, while before the C1 crater impacting. The ejecta deposits of the C1 crater, where CE-3 landed, were wholly derived from the Eratosthenian basalts and some of the Eratosthenian regolith, and this layer supports most of the observed geologic terrains observed along the transverse of the Yutu rover. A subsequent regolith layer was developed on the basis of the ejecta deposits of the C1 crater. Therefore, the subsurface structures at the CE-3 site could be schematically revealed to be layered with three regolith layers, one ejecta material layer and two mare basalt layers at certain depth.

Methods: We use the morphology (i.e., normal, flat-bottomed and concentric) and size of small fresh craters (10–250 m in diameter) on LROC NAC image to determinate the lunar regolith thicknesses at the subsurface of CE-3 landing site [4]. Laboratory experiments suggested that fresh normal craters can constrain the lower limit of regolith thickness (between *D*/4.2 to *D*/3.8, where *D* is the crater diameter), and concentric craters constrain the upper limit (between *D*/10 to *D*/8). The McGetchin's algorithm [5]:

$$t = 0.14 \times R^{0.74} \times (r/R)^{-3.0},$$

was employed to calculate the ejecta deposit thickness at the CE-3 site, where *t* is the ejecta thickness, *R* is the crater radius, and *r* is the radial distance from the crater center. The mare basalts thickness was deter-mined by the excavation depths of large craters and composition of crater ejecta materials [6].

Results: *Regolith thicknesses.* We chose a 5×5 km square areas on LROC NAC frame M1129602407L at the landing site to perform the morphology study and size-frequency distribution measurement of small fresh craters (Fig. 1). Crater counting results indicated that over 90% of fresh craters with diameters less than 21 m were normal craters, and over 90% of fresh craters with diameters larger than 57 m were concentric. The average regolith thickness on the top of the Eratosthenian basalt was thus estimated as 5–6 m, which is consistent with the result of Fa et al. (5–7 m, [7]), and Shkuratov and Bondarenko (~6 m, [8]). Using the same procedure, the average regolith thickness at the northern Imbrian basalt was estimated as 6–7 m. The subsurface regolith thickness on the top the Imbrim basalt was calculated as difference between the thicknesses of the two regolith layers, i.e., ~1 m. Few flat-bottomed and/or concentric craters were visible on the continuous ejecta blanket of the C1 crater, we alternatively referred to excavation depths of small craters (several to tens of meters in diameter) on CE-3 landing camera image to make an approximate estimation for the surficial regolith thickness (Fig. 2), i.e., ~1 m.

Eratosthenian basalt thickness. We investigated the reflectance spectral characteristics for all craters >400 m in diameter surrounding the CE-3 landing site and measured their rim-to-rim diameters (Fig. 3). Whether or not they have penetrated the uppermost Eratosthenian medium-titanium basalt unit was judged referring to the titanium content of ejecta materials using the SELENE MI TiO_2 content map (9). The thickness of the Eratosthenian basalt unit was constrained by the excavation depths ([10]) of these observed craters, which is 45–48 m, well consistent with previous results of both Schaber et al. (30–35 m, range 10–63 m, [11]) and Hiesinger et al. (32–50 m, +11/-5 m, [12]).

Ejecta deposits thickness. We extracted nine radial topography profiles across the C1 crater center from the SELENE TC DTM topography data with 20° increments (Fig. 4). The distances between the two regional highest points on each profile were averaged as the crater diameter, i.e., ~475 m (Fig. 4a). The distance of CE-3 site from the rim crest was measured as ~45 m on LROC NAC frame M102285549L (Fig. 4b). The ejecta deposits thickness at the CE-3 site was thus estimated as ~5 m [5].

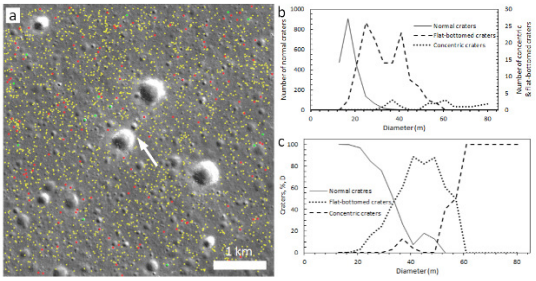

Fig. 1. (a) Crater counting at the CE-3 site for determining regolith thickness, with yellow dots for normal craters, red for flat-bottomed, and green for concentric. (b) Absolute counts and (c) percentage for the three types of crates at each diameter interval *D*.

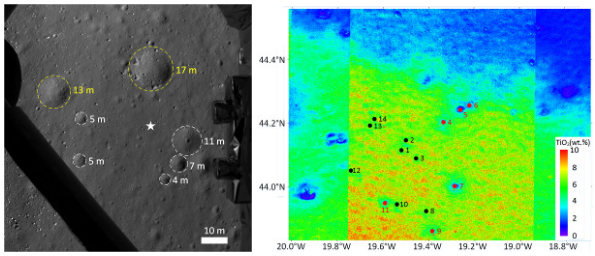

(left) **Fig. 2.** Observed craters on the continuous ejecta blanket of C1 crater for estimating surface regolith thickness. The yellow circles are craters that have penetrated the surface regolith layer, while the whites are craters failed to penetrate. The context image was taken by CE-3 landing camera.

(right) **Fig. 3.** Investigation of craters for calculating the Eratosthenian basalt deposit thickness on SELENE MI TiO_2 content map.

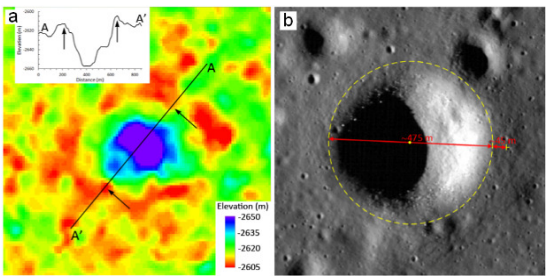

Fig. 4. (a) A sample of radial elevation profiles on SELENE TC DTM data shows regional maximum values (denoted by black arrows) inferred as the rim crest position. (b) Measurements of the crater diameter and distance of CE-3 site from crater rim on LROC NAC frame M102285549L.

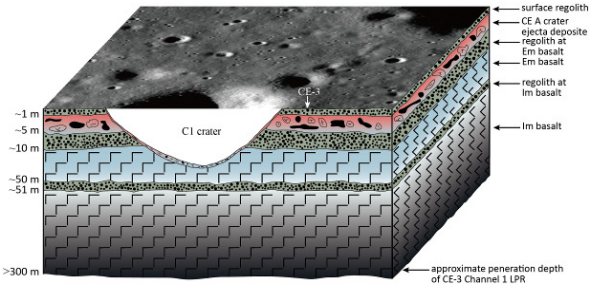

Fig. 5. Schematic subsurface structure model of the CE-3 landing site. The model is not mapped in geometry scale in both vertical and horizontal.

Conclusions and Discussions: Based on the estimated thicknesses of the three regolith layers, ejecta deposits, and Eratosthenian mare basalt unit, a schematic multi-layered subsurface structure model of the CE-3 landing site was illustrated (Fig. 5). Our results could serve as essential references for the on-going interpretations of the CE-3 radar data. The mutual validation between of results of this study and CE-3 radar observations will strengthen methods for quantifying lunar subsurface structure using crater morphologies and scaling.

Acknowledgements: L. Qiao acknowledges Dr. Wenzhe Fa and Ms. Tiantian Liu for instructions on calculating regolith thickness. This work was supported by the Key Research Program of the Chinese Academy of Sciences (No. KGZD-EW-603), the Natural Science Foundation of China (No. 41373066, 41403053).

References: [1] Zhao J. et al. (2014) *Sci. China. Phys. Mech., 57,* 569-576. [2] Xiao L. (2014) *Nat. Geosci., 7,* 391-392. [3] Zhao N. et al. (2014) *Sci. China. Phys. Mech., 57,* 2345-2353. [4] Oberbeck V. R. and Quaide W. L. (1967) *JGR, 72,* 4697-4704. [5] Mcgetchin T. R. et al. (1973) *EPSL, 20,* 226-236. [6] Thomson B. J. et al. (2009) *GRL, 36,* L12001. [7] Fa W. et al. (2014) *JGR, 119,* 1914-1935. [8] Shkuratov Y. G. and Bondarenko N. V. (2001) *Icarus,* 149, 329-338. [9] Otake H. et al (2012) *LPSC XLIII,* Abstract #1905. [10] Melosh H. J. (1989) Impact Cratering: A Geologic Process, 78. [11] Schaber G. G. (1973) *LPSC IV,* 73–92. [12] Hiesinger H. et al. (2002) *GRL, 29,* 1248.